Spring 2012

The effects of cyclic hydrostatic pressure on chondrocytes in an alginate substrate

Brice James Journot
University of Iowa

THE EFFECTS OF CYCLIC HYDROSTATIC PRESSURE ON CHONDROCYTES IN AN ALGINATE SUBSTRATE

by

Brice James Journot

A thesis submitted in partial fulfillment
of the requirements for the Master of
Science degree in Biomedical Engineering
in the Graduate College of
The University of Iowa

May 2012

Thesis Supervisor: Assistant Professor James A. Martin

Graduate College
The University of Iowa
Iowa City, Iowa

CERTIFICATE OF APPROVAL

_____

MASTER'S THESIS

_____

This is to certify that the Master's thesis of

Brice James Journot

has been approved by the Examining Committee
for the thesis requirement for the Master of Science
degree in Biomedical Engineering at the May 2012 graduation.

Thesis Committee: _____
James A. Martin, Thesis Supervisor

_____
Sarah C. Vigmostad

_____
Prem S. Ramakrishnan

_____
Edward A. Sander

ACKNOWLEDGMENTS

Firstly, I would like to thank Dr. James Martin. Without his generous support from the Orthopaedic Biology lab, I would not have been able to pursue the work presented here, nor the future opportunities that a graduate education can provide. Thanks, Jim.

I also owe a debt of gratitude to Dr. Prem Ramakrishnan. His guidance and assistance have been invaluable to me every step of the way, from bouncing design ideas off of to giving me council during the writing of this thesis. If I let him, he'd probably try to do all my work for me (and we can't have that). Thank you for all your help, Prem.

Throughout both semesters of this (sometimes grueling) test of graduate education, my friend and labmate Marc Brouillette has always been there. There's nothing quite like having a friend down in the trenches with you to help get you through what seem like some of the most stressful times of your life (to date). Oh, the times we had solving math problems only a computer should handle. I've leaned on him more than once for support, and for that, I thank you buddy.

I'd like to thank the entire Orthopaedic Biology lab, especially Abbie Lehman, for showing me the ropes on the basics and without whose tireless effort would probably cause the lab to grind to a halt. Also, Barbara Laughlin (Rhubarb) for her assistance obtaining and isolating chondrocytes; Hyeong Choe for his culturing of CPCs; and last, but certainly not least, Theresa Messlein for her unending support and the assistance she provided proofreading this document. I greatly appreciate everything you all have done.

I would conclude by thanking my parents, who's (sometimes harsh) life lessons have helped forge me into the person I've become, and shown me that when you set your mind to the task, you can never fail. Thank you.

TABLE OF CONTENTS

LIST OF TABLES

Table

LIST OF FIGURES

Figure

CHAPTER 1

INTRODUCTION

Osteoarthritis is a debilitating musculoskeletal disease for which there is currently no cure. In all of its forms, it affects nearly one third of the US population with a combined annual financial cost of approximately $105 billion[8]. Patients with osteoarthritis range in age from young adults to the elderly. Treatments acceptable for the less-active elderly population, such as joint replacement or fusion, are not feasible for younger, more active patients [10]; thus, treating osteoarthritis in the young is particularly challenging. Osteoarthritis in this population is primarily associated with joint trauma and its sequelae, which often include abnormal joint mechanics. Unfortunately, the relationships between joint mechanics and the pathogenesis of post-traumatic osteoarthritis are complex and have yet to be clearly defined [12]. This gap in knowledge has contributed to the lack of treatment options to reduce the risk for trauma-related osteoarthritis, which has not changed despite considerable refinement in surgical procedures.

While osteoarthritis is an organ-level degenerative disease that affects the entirety of a joint, it is articular cartilage degeneration and loss that most directly impairs function. Regular, moderate mechanical loading is essential to cartilage and joint health; however, excessive loading that exceeds maximal stress limits may cause focal lesions. These lesions initiate the progressive degeneration of cartilage surfaces throughout the joint—a hallmark of end stage osteoarthritis[9].

Intrinsically, cartilage has poor regenerative potential; it is both avascular and aneural, and has a low cell density compared to other tissues[59]. A specialized cell type,

the chondrocyte, constructs and maintains the extracellular matrix throughout life. The cartilage matrix is a specialized, water-binding, viscoelastic material that is well-adapted to resist compression at physiologic stress rates. Injuries to the matrix elicit responses from a second cell type, the chondrogenic progenitor cell, which migrates to the injury site and proliferates in a largely futile effort to repair the damaged matrix[15,37,52].

Cartilage's poor repair potential has prompted a need to produce artificial cartilage ex vivo. The cartilage engineering problem is complex and requires a multifaceted approach combining biology, mechanics, and systems engineering. Advances in culture systems, scaffolds, and seeding strategies have produced constructs containing cells embedded in an extracellular matrix, but with only a fraction of the mechanical durability of native tissue[19,36]. Mechanical stimulation may be required to increase the resilience of the tissues, in addition to these biologic factors. There are several modes of mechanical stimulation, including shear, direct unconstrained compression, and hydrostatic stress.

Hydrostatic pressure has been identified as one of the most important forms of loading in cartilage mechanics[51], and a variety of mechanically-active culture devices have been implemented. Generally speaking, static hydrostatic pressures of any magnitude inhibit the synthesis of cartilage matrix (chondrogenesis) by chondrocytes and chondrogenic progenitor cells (CPC) in monolayer[21, 33, 56]. However, the results are varied among three dimensional constructs, with super-physiologic pressures usually resulting in inhibition of chondrogenesis[25, 38, 47], while pressures in the physiologic range produce varied effects[17, 25]. Cyclic hydrostatic pressures stimulate chondrogenesis in chondrocytes and CPCs in both two-dimensional[26, 43] (cell monolayer) and three-dimensional[19, 29, 36, 60, 61] (construct) environments. However, it is unclear whether the full

benefit of cyclic pressure regimens has been exploited. Few systematic optimization studies have been undertaken, in part because of the daunting number of potentially significant experimental variables (culture model, pressure parameters, treatment frequency and duration, etcetera). The expansive study designs required to explore even a handful of the potential combinations of such variables creates a great need for high throughput testing systems. Furthermore, because monolayer-cultured cells, three-dimensional scaffold cultures, and intact cartilage explants all have value as experimental models, there is a need to accommodate a wide variety of sample sizes and geometries.

The proposed hydrostatic pressurization system is extremely versatile. A flexible membrane specimen pouch allows the stimulation of any sized specimen, from cells through small joints. The modular design allows the system to be driven via any type of linear actuator (stepper-motor, servo, hydraulic piston) and the chamber is designed to safely accommodate pressures up to 25 MPa, with a minimum burst pressure of 55 MPa. Controlling software has been simplified as much as safety allows, and can currently generate a waveform of up to four linear parts, with the ability to program more parts as desired. Individual tests can be run for as long as the experimental protocol requires. Operation requires only a rudimentary knowledge of computing, which can minimize the learning curve and mistakes.

Utilizing this system, various experimental models have been tested. The current study uses alginate beads seeded with normal chondrocytes. We sought to confirm the stimulatory effects of cyclic hydrostatic stress on chondrogenesis (extracellular deposition of proteoglycans and collagens) in articular chondrocyte cultures.

CHAPTER 2

BACKGROUND AND SIGNIFICANCE

Significance

Among musculoskeletal diseases, there are few as debilitating and prevalent as post-traumatic osteoarthritis (PTOA). The economic and societal burdens of the disease are difficult to determine due to the lack of a clear clinical definition and objective population data, but Brown et al have estimated that approximately 12% of all symptomatic osteoarthritis (OA) is due to PTOA of the hip, knee, or ankle . As of 2006, this accounts for 5.6 million Americans and $3.06 billion annually in financial costs[8]. The disease has a diverse demographic, with patients presenting from the young to the elderly. While those in the elderly range (60+) can usually be treated successfully with joint replacement/fusion and restriction of activity, these modalities are not acceptable or feasible for many young and middle-aged patients, leading to a complex clinical problem[10]. Currently, there is no cure for OA, and although many studies have shown that joint injury leads to joint degeneration, understanding of the mechanical and biological aspects of the disease remains limited.

The burdens of PTOA reach beyond the societal financial cost and have a debilitating impact on the quality of life for patients. Studies show that severe PTOA affecting the ankle not only leads to decreased joint function, but also a decrease in general health status[39]. Greater injuries require more intensive surgical and treatment modalities; the more complex the treatment, the higher the likelihood of complications which could lead to permanent morbidity[14]. Anderson estimates that, even with the best

current care available, 40% of those with significant meniscal/ligamentous tears or articular surface injury still develop OA in the affected joint[1]. Other than attempts to restore joint stability, congruity, and alignment, there are currently no treatments that decrease the risk, nor slow the rate of progression, of PTOA[10].

While there is considerable experimental, clinical, and epidemiological data which suggest one of the major causes of OA is joint loading that exceeds the tolerance of the articular surface, mechanistic relationships between OA and mechanical stress levels have yet to be defined[12]. Joint stability, joint incongruity, and patient age play a role in the progression of the disease. Martin and Buckwalter's work with chondrocyte senescence suggests that as chondrocytes age, they become less responsive to mechanical stimuli, secrete less glycosaminoglycans (GAGs), and are less effective at repairing articular surface insults[40]. A better understanding of the mechanical and biological relationships that control the outcomes of PTOA will aid in development of more effective treatments for the disease.

Background

Articular Cartilage and Osteoarthritis

Macro-scale

Articular cartilage is an avascular tissue whose primary function is the distribution and absorption of mechanical force caused by the actuation of diarthrodial joints. The hyaline cartilage which covers articulating joints has an extremely low coefficient of kinetic friction, and its composition allows it to passively distribute compressive loads with great efficacy[53]. However, it is this same composition that is responsible for cartilage's poor repair characteristics.

While hyaline cartilage is found in some cartilaginous joints, it is predominantly located in the capsules of synovial joints. Synovial joints are those that envelop two or more articulating bones, surrounded by an articular capsule and filled with a lubricating fluid known as synovial fluid. A diagram of a synovial joint is shown in Figure 2.1. The mechanical system created between the articular cartilage and the synovial fluid is the cause of articulating joints' low-friction motion[53]. The synovial fluid is also a transport medium by which the joint cartilage receives oxygen and nutrients.

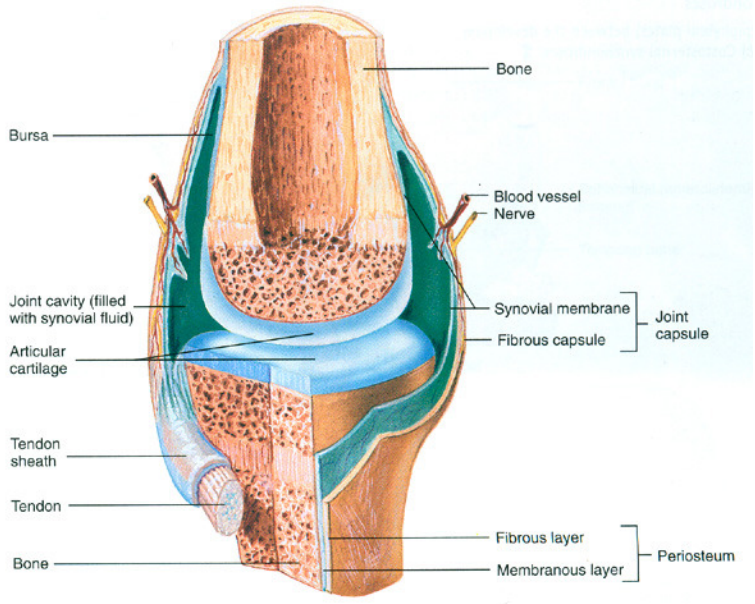

Source: http://www.bcnlp.ac.th/Anatomy/page/apichat/bone/picture/synovial-joint001.jpg

Figure 2.1: Articulating joint anatomy.

Articular cartilage is a biphasic tissue comprised of a solid as well as fluid phase[45]. The fluid phase gives the cartilage its ability to distribute and resist compressive

loads. The solid phase is comprised of a matrix of collagen fibers and proteoglycans (PG) (greater than 95%) embedded with a specialized cell type, the chondrocyte, which make up only 1-5% of the phase[58]. The fluid phase consists of the extracellular water within the solid matrix.

The mechanical loading experienced by articular cartilage has a direct effect on joint health. Wolff's law states that the form of a tissue is dictated by its function, and any alteration of the tissue environment will elicit form changes of the tissue. Indeed, it has been shown that prolonged immobilization of synovial joints has detrimental effects, including reduced proteoglycan (PG) content and rate of synthesis of new cartilage tissue[6]. The reverse has also been shown: an increase in the amount of loading, as is seen in moderately active runners, leads to an increased cartilage thickness, increased PG content, and higher indentation stiffness when compared to normal non-runners[11]. It is not only the magnitude of loads that affect how the joint responds, but also the rate at which these loads are applied. Slowly applied loads allow the interstitial fluid within the matrix to migrate and distribute the force; rapidly applied impulse loading does not allow this migration and can create regions of high local stress, rupturing the matrix[14]. In either case, extreme mechanical loading that causes direct or indirect impacts, joint capsule and/or ligament/meniscal tearing, joint dislocations, or articular fractures can trigger a cascade of events that leads to joint degeneration and osteoarthritis[10].

Osteoarthritis (OA) is a disease of synovial joints characterized by joint pain and dysfunction. It affects articulating joints that have undergone degeneration at the level of the organ (joint-wide), and has multiple risk factors including age, genetic and developmental aberration, and injury to the joint[10]. Epidemiologic studies indicate that

mechanical stresses which exceed the articular surface tolerance, either acutely or over repetition, have a role in the progression and development of OA[8].

OA that develops secondary to acute joint trauma is called post-traumatic osteoarthritis (PTOA). This secondary type of osteoarthritis results from the mechanical insult to the joint as well as the biological events occurring post-injury. These events may differ depending on the level and type of tissue damage present after an injury. Buckwalter has identified three distinct types of cartilage damage, each with different healing characteristics[9]. Injuries to the cartilage matrix and cells with no visible disruption of the articular surface may restore the normal tissue composition if the basic matrix structure remains intact; else, the lesion may progress to degeneration. In injuries with visible articular surface disruption, such as chondral ruptures, healing is dependent on location and size of the lesion, and joint stability and alignment. Those injuries forceful enough to cause bone as well as cartilage disruption, as seen in osteochondral fractures, depend on the location and size of the lesion as well as joint mechanics (stability and alignment)[9]. If the joint becomes osteoarthritic, current treatments attempt to restore normal joint alignment and stresses, as instability and excessive joint stress is believed to exacerbate OA progression.

Micro-scale

It was previously believed that cartilage had only one specialized cell type, the chondrocyte, but current work has shown that cartilage actually contains at least two distinct cell types, the second of which is the chondrogenic progenitor cell[15,23,35,37, 52].

The articular cartilage micro-structure and organization are what grant the tissue its mechanical properties. It can be divided into four horizontal layers: the superficial,

transitional (middle), deep, and calcified zones[31]. Each zone has different constituents and organization which play a role in the overall properties of the tissue. The superficial zone is the thinnest zone, about 10-15% of the overall thickness. It has the highest water and chondrocyte content, a low PG content, and is densely packed with collagen fibers running parallel to the surface; the chondrocytes in this region are disc-like in shape. Middle zone (40-60% overall thickness) chondrocytes are spherical, and the zone's PG content is increased when compared to the superficial zone with collagen fibers that are randomly aligned. In the deep zone (30% overall thickness), chondrocytes are arranged into columns perpendicular to the surface; cell density and water content are lowest, PG content highest, and contains collagen fibers arranged perpendicular to the surface. The deepest zone, the calcified cartilage, is separated from the other zones by the tidemark, a band of fibrils visible at the base of the deep zone. The calcified cartilage contains rounded chondrocytes and lacks PG[31].

Chondrocytes are responsible for producing the constituents of the specialized matrix of cartilage, such as PG, collagens, and other proteins. The different layers of cartilage contain different relative amounts of these proteins, and the localization of the cell determines its metabolic activity. Superficial zone chondrocytes create more collagen (than the other zones) and less PG, whereas deep zone cells create a larger amount of PG[46] with less collagen. Chondrocytes are sequestered in lacunae, small cavities in the matrix that typically house only one cell. The lacunae are widely spread, and cartilage has a relatively low cell density compared to other tissues—on the order of 10,000 cells per cubic millimeter in adult femoral head cartilage[59]. This low cell density may be a product of the avascular environment. The limited amount of nutrients and

oxygen available may impose an upper limit on the number of cells per volume unit of cartilage tissue. Chondrocytes are able to thrive in low oxygen tension (as low as 1%), and produce a majority of their ATP through glycolysis. They arrest their cell cycle once mature, and only divide under the effect of pathology or an injury state[3]. This longevity could be a factor in chondrocyte senescence, which leads to a loss of the cells' ability to maintain and restore the articular matrix. The process of chondrocyte senescence may also explain the age-related increase of OA in older patients[40].

The study and effects of chondrogenic progenitor cells (CPC) have only recently started taking a larger role in OA. These cells are observed in OA and injured cartilage[37], as well as healthy cartilage[27]. CPCs are sometimes referred to as migratory progenitor cells because of their ability to migrate towards an injury site[37]. Found in the superficial zone of articular cartilage, CPCs exhibit progenitor-like characteristics, including the ability to form colonies from low seed densities and multipotency[15]. Seol has shown that the migration of CPCs across the cartilage is controlled, at least in part, by chemotaxis, with chondrocyte lysates producing the most marked (significant) increase in migratory potential. In addition, the gene expression of CPCs shows substantial phenotypic differences between that of chondrocytes and mesenchyaml stem cells (MSC)[52], suggesting these cells have a distinct function.

Cartilage Tissue Engineering

The task of engineering a functional, viable cartilage tissue construct is complex, requiring a multidisciplinary approach that incorporates biology, mechanics, and engineering. This is due to the complex nature of the tissue. Articular cartilage undergoes large compression forces with high frequency yet remains resilient and robust;

these qualities are associated with the unique extracellular matrix (ECM) composition within the tissue. Thus, any strategy with the goal of producing functional cartilage tissue must incorporate methods to control matrix characteristics and mechanics, in addition to cell viability and growth.

There are several different aspects of the tissue engineering problem. Some groups opt for no mechanical stimulation, and instead focus on biological growth of constructs. For example, using self-assembly on agarose substrate, Hu and Athanasiou have developed constructs reaching approximately 40% the stiffness of native juvenile bovine cartilage after 12 weeks' culture[30]. It has also been observed by Bian et al that co-culturing MSCs together with chondrocytes (in hyaluronic acid gels) results in constructs with a significantly higher elastic modulus, as well as higher glycosaminoglycan levels, than either cell type cultured alone[5]. The temporal effects of growth factor stimulation have been explored by Ng et al, who have found that the removal of growth factors after 14 days culture results in constructs with significantly higher compressive properties and collagen content (at 28 and 42 days) than constructs continuously cultured with growth factors[49]. Others have focused on the importance of the interface boundary between the cartilage and bone (the calcified cartilage zone). One group report that by growing a zone of cartilage in mineralizing medium (mimicking the calcified cartilage zone) increases of 3.3 fold (up to 670 kPa) can be achieved in interfacial shear stiffness[57]. However, this value still falls significantly short of the estimated 2.6 MPa shear modulus of articular cartilage[51]. Erickson et al have also studied the factors that determine integration strength of constructs using MSCs in methacrylated or agarose gels, noting that constructs that were pre-matured before implantation were more chondrogenic than

those without a pre-maturation period[20]. Still others study the oriented nature of cartilage tissue, and have shown that decellularized and oriented ECM scaffolds cultured with MSCs have a compressive modulus of 89.35 kPa, 2.5 times that of non-oriented ECM scaffolds[32]. While promising, each of these results only addresses one specific piece of the cartilage engineering problem, and all show mechanical properties below that of native tissue.

Mechanical stimulation of biologic constructs is an avenue of study that has received great attention in the past 20 years. Shear, compression, and hydrostatic pressurization can be realized separately with a dedicated system; systems employing two of the stimulation methods have been used (for example, hydrostatic compression with perfusion[44]) albeit rarely. Heath and Margari have described the typical cartilage loading process as a rolling movement of direct compression, together with a generation of shear and tensile force components, and a high hydrostatic pressure[28]. Using this definition as a template, it can be seen that each of the currently employed systems fulfills a specific step in the loading cycle.

Cartilage undergoes axial direct compression during all types of normal loading cycles. Direct compression systems typically have a base or jig which allows the fixation of one or more samples (explants, constructs) and a controllable force applicator, with the components contained in a suitable tissue environment. Sauerland et al. have developed a piston-driven force applicator that allows the fixation of cartilage explants inside a polyethylene-lined titanium vessel, immersed in a small amount of culture medium[50]. Our group has performed similar work (unpublished to date) on static and cyclic direct compression loads, using a stepper-motor force applicator with loadcell feedback and an

explant clamp jig. The entire system can be placed in a medium-size incubator to control for temperature (37º C), humidity (90-100%), and oxygen tension (5%).

Shear systems are one of the simpler mechanical stimulation methods, and can be realized by fixing tissues/constructs in culture dishes, immersed in media, and placed on an orbital shaker[22]. A second approach utilizes spinner flasks, or comparable vessels, with a magnetic stir bar and constructs fixed to inner walls of the vessel[7]. The imparted shear forces are a function of the velocity and (Newtonian) fluid properties of the culture medium; thus, greater shearing can be achieved, with these systems, by a faster shake/spin or a more viscous fluid, as illustrated in the following fluid shear equation:

$$\tau = \mu \frac{\partial u}{\partial y}$$

where τ is the magnitude of the shear stress in the x-direction (or direction normal to y), μ is the dynamic viscosity of the fluid, u is the velocity of the fluid, and y is the distance above the boundary (for boundary shear stress, y is evaluated at 0). Systems that impart a low shear stress by circulating culture media through a loop (and over constructs) are known as perfusion systems, and are a sub-type of the shear modality.

The application of hydrostatic pressure (HP) on cartilage has gained attention over the past few decades. During loading of *in vitro* as well as *in vivo* tissue, the pressurization of interstitial fluid supports a great majority of the applied compression forces, with less than 10% of the force actually directly compressing the solid phase (matrix)[16]. Along with similar findings, this may mean that hydrostatic pressure is the most important load experienced by the joint[51]. Hydrostatic devices come in a variety of modes, and the results to date show that the interactions between magnitude, frequency, duration, and loading regime have markedly different effects on cartilage.

Hydrostatic Pressure

Broadly, hydrostatic pressure can be divided into two categories: static and dynamic. Practically, static pressure can be defined as an application frequency of near-zero Hz (less than 0.001 Hz). Dynamic application has two subgroups, cyclic (application with a regular frequency) and intermittent (application with irregular frequency). Due to the confusion that can be caused by classifying one strategy as "dynamic hydrostatic", dynamic analyses will be referred to as cyclic or intermittent, depending on the periodicity of the application.

Micro-environment plays a large role on the effects HP systems impart on specimens. In general, cell monolayers seem to react favorably (more chondrogenic) to cyclic and intermittent stimulation[26, 43], while static application has no or a repressive effect[21, 33, 55]. Three dimensional cultures show favorable reaction to cyclic stimulation[19, 29, 36, 60, 61], and also to static stimulation[17, 25]. However, the variability of results to date in three dimensional cultures suggests that more work is needed to optimize the duration, frequency, magnitude, waveform, and application timing of each of the experimental models, both dynamic and static.

Cell monolayers show little to no benefit from application of static HP. In fact, Fioravanti et al. have reported that after three hours of 24 MPa static HP, normal human chondrocytes exhibit increased organelle disorganization, fewer mitochondria, and a cytoskeletal arrangement of actin and tubulin consistent with that seen in osteoarthritic human chondrocytes[21]. Other studies show that static HP of physiologic levels (5-10 MPa, 4-20 hours) has no effect on sGAG incorporation and a decrease in collagen mRNA levels[33,56]. These results are quite different from those utilizing cyclic HP. Broadly,

Hansen et al. note that intermittent application of HP on chondrocytes in culture shows an additive effect on proliferation, collagen secretion, and phenotypic stability with reduced oxygen tension, and that these effects are reversible[26]. The effects are not only limited to differentiated chondrocytes in monolayer; using ovine MSCs, Miyanishi et al. demonstrated that cyclic HP of 1 and 10 MPa, at 1 Hz, increases GAG production while 0.1 MPa (sub-physiologic) does not[43].

The optimization problem becomes even more complex in three dimensional constructs, where cell attachment, environment, and matrix conditions—as well as a new variable, application time frame—all contribute to the tissue reaction. Hall et al. have demonstrated the effects of duration and magnitude of static HP on explants, observing that a 20 second to 5 minute application of 5-15 MPa (mid-high physiologic) shows increased proline incorporation; conversely, two hours of 20-50 MPa static HP (super-physiologic) lead to a decreased proline incorporation versus unloaded controls[25]. It is also beginning to become clear that the temporal aspects of static HP, namely the timing and duration of application, are important. Bovine chondrocytes seeded into agarose gels respond optimally to 10 MPa static HP when it is applied from 10-14 days after seeding, showing maximized increases in GAG and collagen content, and an increase in aggregate modulus[17]. Similar studies show that chondrocytes seeded into alginate beads and pressurized within 24 hours at 50 MPa static HP have suppressed GAG, PG, and collagen II content, and have significantly higher rates of apoptotic cells (as high as 60%) than beads allowed to culture for two weeks prior to the same stimulation[38, 47]. 10 MPa caused a similar apoptotic trend, but with a reduced impact (20% apoptosis)[47]. These findings suggest that the presence of an extracellular matrix in a three dimensional environment

could shield chondrocytes from the harmful effects of excessive HP stimulation; a corollary is the finding that the solid phase (matrix) of cartilage absorbs much of the remaining hydrostatic pressure when loaded physiologically and does not deform a measurable distance[4]. Thus, cells that have no matrix, or a matrix different from the normal ECM, may undergo abnormal stresses/strains in the presence of prolonged static HP and react by becoming more osteoarthritic or apoptotic.

Contrary to the varied effects of static HP application, cyclic HP generally creates a favorable chondrogenic environment. Human chondrocytes cultured in alginate beads have displayed chondroprotective gene expression (downregulation of collagen I and MMP-13) when stimulated with 5 MPa, ½ Hz HP for 3 hours per day[61]. Knight et al. have shown that chondrocytes in agarose stimulated by either static or cyclic 5 MPa (1 Hz) for two hours displayed significant rearrangement of actin elements immediately following loading[36]. However, after 60 minutes the statically loaded cells returned to their prior-loading state, whereas the cyclic cells showed a further increase in actin remodeling (into a punctate organization)[36]. Even in sub-physiologic models (0.3 MPa) , chondrocytes in alginate beads show a 25% increase in the GAG/DNA ratio, and a 65% increase in the collagen II / collagen I ratio[29]. Cyclic HP also has chondroinductive properties, as several groups have shown a phenotypic shift (increased collagen II and aggrecan expression, reduced collagen I) of MSCs subjected to 1-5 MPa cyclic HP at 1 Hz[19, 60]. Neonatal dermal fibroblasts also respond in a chondrogenic fashion when exposed to 5 MPa, 1 Hz cyclic HP; Singh et al. have seen that after 7 days, collagen I production decreases markedly, and after 21 days collagen II production was upregulated[54].

There are many different systems and experimental models used to apply HP with the goal of increasing chondrogenic potential, both with and without scaffolding materials. It may be that there are several methods to obtain a satisfactory cartilage construct; however, the current models must be optimized. Further work should focus on system-model optimization.

CHAPTER 3

SYSTEM DESIGN AND RATIONALE

Project Parameters

Before beginning any design work, agreement upon project goals, constraints, and specifications was necessary. This process built a project concept upon which designs could be focused, limits set on cost, and provided a foundation for future design revisions. The overarching goal of the project was to design a simple, cost-efficient experimental system which could mechanically stimulate orthopedic tissues, cells, and constructs via hydrostatic pressure, with an ultimate goal of using the system, in parallel with other techniques, to manufacture functional cartilage tissue implantables.

The requested pressure range was from 0 to 5 MPag (MPa gauge), allowing sub-physiologic to mid-physiologic stimulation (in reference to the knee joint). Articular cartilage undergoes high compressive forces during use. These compressive and tensile forces pressurize the interstitial fluid in the extracellular matrix, which then exerts a hydrostatic stress on the surrounding tissue. The system pressure range was designed to represent these hydrostatic pressure fluctuations.

Biologically, the system needed to mimic, as closely as possible, the conditions under which joints function. The major factors considered were temperature, oxygen tension, nutrition, and humidity. Joints are avascular tissues in an aqueous environment, and gain their nutrition through diffusion and convection. A low oxygen tension (1-5% O_2) at 37° C immersed in culture medium provided this biomimetic environment. The system also needed to be sterile, in an effort to eliminate infection and contamination. A

design constraint that was eventually lifted was the ability to fit the entire assembly inside a mid-size incubator. It was initially thought that in order to simulate biologic conditions, an incubator was necessary. When flexible membranes were introduced (satisfying the oxygen tension requirement by sealing conditioned media in gas-impermeable pouches), a water bath became sufficient in providing the temperature requirement.

The system had several operational and technical requirements, among which were throughput, ease of use, and accuracy and precision. To facilitate usage, software controls were kept as autonomous as possible, allowing user input only when absolutely necessary (such as during specimen information input or motor mounting). In addition to minimal user interaction, those areas requiring a response or action were detailed with step-by-step instruction, allowing a person unfamiliar with the system to use it effectively. Mechanically, the setup process was kept to as few steps as possible, both to reduce operating errors and minimize time costs during experimentation. Batch processing also helped to reduce unnecessary setup time by increasing the number of specimens that could be tested during one operation; the minimum required count was five of the largest specimens--1 inch by 1 inch by ¾ inch explants--typically tested in our lab. To validate specimens were indeed getting the prescribed dose of hydrostatic stress, direct measure feedback needed to be incorporated. The simplest way to implement this was to include a pressure transducer. Direct feedback would allow for precise software control, and controller accuracy within ±10% of the prescribed pressure magnitude was decided as appropriate.

Low material, setup, and manufacturing cost were critical factors in the design. Cost-benefit analyses were to be performed for any sizable design choice, and the

decision to keep manufacturing costs as low as possible while maintaining a high level of user and setup simplicity affected many of the final designs.

Determination of Pressurization Mode

Within cartilage engineering, there are three main modes that are used to apply a hydrostatic load to the developing construct (as defined by cells, cell-seeded scaffolds, or explanted tissues). These systems can be classified as indirect-, direct-, or flexible membrane fluid-driven[51]. Each mode possesses strengths and weaknesses, and thus each system performs well under a specific set of operational parameters and goals.

Indirect systems utilize a gas phase to apply pressure to constructs via hydrostatic pressure transmission through a liquid phase (such as culture medium). A schematic of a simple pneumatic indirect pressure system is illustrated in Figure 3.1. These systems are versatile, relatively simple to construct and operate, and work well for projects that require lower hydrostatic pressures. Limitations can arise when using pneumatics at higher pressures due to the dynamic reliability and resolution of regulators as well as the feasibility of high-pressure inert gas sources.

Direct systems are those which pressurize the liquid immediately surrounding the constructs (usually culture medium) without the use of a secondary fluid phase. These systems are typically realized via hydraulics; Figure 3.2 shows a block diagram of a simple hydraulic system. Since the pressure is generated via motor force as opposed to gas concentration, much higher pressures can be realized, up to the safety limit of the vessel in use--though in cartilage stimulation and testing, the range is roughly 0-50 MPag (MPa gauge) representing sub-physiologic to super-physiologic stresses. Precise

hardware and software control make the reliability of these systems high, and a material testing machine (MTS) may be utilized to drive the pressure.

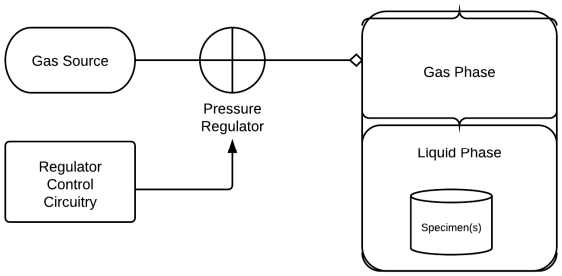

Figure 3.1: Block diagram of indirect pneumatic system.

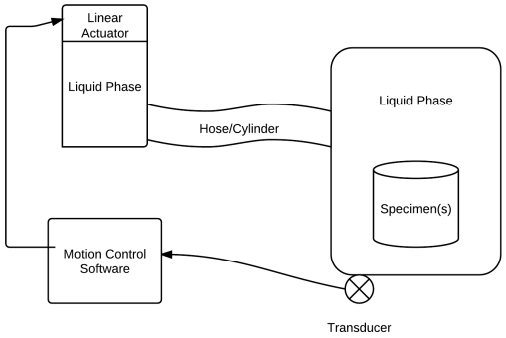

Figure 3.2: Block diagram of simple hydraulic direct system.

Direct mode systems are usually more expensive to produce, as the attainable pressures warrant further safety parameters integrated into the vessel design and extensive seal mechanisms must be in place. They also require sterilization following each use, since the constructs are in direct contact with the pressurizing fluid and thus the chamber itself.

Flexible membrane mode is a hybrid-of-sorts between direct and indirect pressurization, and uses flexible membranes that transmit pressure between the contained constructs immersed in media, and an external pressurization fluid. This mode can be driven with either pneumatics or hydraulics, and mitigates many of the limitations of the previous two systems. Since the constructs are sealed within flexible membranes, no contact with the vessel ever occurs and time spent sterilizing equipment, as well as volume of media, can be reduced. They can also be hydraulically-driven, which allows for high reliability and a robust operating pressure range. Limitations of this mode include the added cost of membranes, and a possible extension to the experimental setup time.

It is important to appropriately choose system specifications based upon the goals of the project, and careful consideration was given to each mode before proceeding with hardware design. Pneumatic systems were decided against due to the unreliability of control systems and handling of gas cylinders. Direct contact mode was also excluded because it had a high material cost due to the large amount of required culture media and sterilization/contamination concerns. Experience with, and availability of, LabVIEW software prompted discussion of linear actuator control (as had been performed in previous work). The decision to use hydraulic drive and minimize material cost bore the innovation of heat-sealed pouches to contain specimens while loading. These pouches

were created using existing lab equipment to minimize cost. Thus, it was decided that a hydraulic, flexible membrane system was the best fit for the constraints of the project.

Vessel

Due to the risk of high pressure rupture, proper care when designing a pressure vessel is of extreme importance. The American Society of Mechanical Engineers maintains a standard for the construction and safe operation of pressure vessels called the ASME Boiler and Pressure Vessel Code (BPVC). This standard covers all pressure vessels that generate an internal pressure greater than 14.7 psi (1 atm). Pressure vessels that generate pressures in excess of 10,000 psi (70 MPa) have special guidelines and standards and are considered high pressure vessels. For this project, the maximum safe operating pressure of the vessel was specified at 25 MPa (3750 psi) and thus was considered a normal pressure vessel. All designs were drafted and drawings created with Pro/ENGINEER Wildfire 5.

Geometric constraints were analyzed using the dimensions of the largest predicted specimens. 1" x 1" x ¾" explants were considered a standard large model specimen, with an approximate volume of ¾ in^3 each. Each explant would be sealed in a flexible membrane (bag) with a media to tissue volume ratio of roughly twenty (approximately 20-25 mL (1.53 in^3) of culture media). This resulted in a volume of 2.3 in^3 per specimen, and bags with a maximum face area of 3.5" x 3.5". Thus, the inner vessel radius was set at 1.75" in order to accommodate the largest predicted bag. This radius exceeded the 5 specimen requirement, allowing 6+ specimens to be loaded simultaneously.

While it is possible to construct a spherical pressure vessel, this is not commonly seen in practice due to the increased cost and fabrication difficulty of spherical

geometries. Cylindrical vessels with flat or hemispherical ends are much more cost efficient, and function adequately under most circumstances. Due to the simplicity of machining a cylindrical vessel with flat ends, this shape was chosen. The stresses endured by a thick walled cylindrical vessel with flat ends are well-characterized by a set of equations known as Lame's Equations[48]:

$$\sigma_r = A + \frac{B}{r^2} \; ; \; \sigma_\Theta = A - \frac{B}{r^2}$$

where σ_r is the stress in the radial direction, σ_Θ is the hoop stress, and A and B are constants of integration which must be solved based upon the boundary conditions. Setting the external pressure to zero, considering all internal pressures as gauge and solving yields the equations:

$$\sigma_r = \frac{r_i^2 p_i}{r_o^2 - r_i^2}\left(1 - \frac{r_o^2}{r^2}\right) \; ; \; \sigma_\Theta = \frac{r_i^2 p_i}{r_o^2 - r_i^2}\left(1 + \frac{r_o^2}{r^2}\right) \; ; \; \sigma_z = \frac{r_i^2 p_i}{r_o^2 - r_i^2}$$

where r_i is the inner radius of the cylinder, r_o is the outer radius, p_i the internal pressure, r an arbitrary radial distance, and σ_a the axial stress (derived by adding the boundary condition of closed cylinder ends). By inspection, it can be seen that the maximum radial stress occurs at the inner radius wall; maximum hoop stress also at the inner radius wall; and maximum axial stress is constant and independent of radial position. Since the internal pressure and inner radius are known (750 psi and 1.75", respectively), the outer radius becomes dependent on the vessel material's yield stress.

Material selection presented further design challenges. General steels were not suitable due to oxidation and corrosion by the aqueous environment (water was used as the external pressurizing fluid due to availability). Stainless steels were viable and desired--however, due to the poor machinability of stainless steel, cost became

prohibitively high. 6061-T6 aluminum with an anodized finish was chosen for the vessel and a majority of the components due to its ease of machinability, high strength, and low cost--less than half the cost of stainless steel.

Wall thickness was found by inserting the tensile yield strength of 6061-T6[41] into Lame's equations and solving for the minimum required outer radius. The calculated outer radius was 1.80" for a total wall thickness of 0.05". Applying a safety factor of 2.5 resulted in a total wall thickness of 0.125". When manufacturing the vessel, stock aluminum was available in 6" diameter; the wall thickness was increased to ½" to minimize machining costs and still leaving the minimum required ¾" flange. This increased the effective safety factor to 10.

Special considerations were made when designing the lid of the vessel. Bolt layout and minimum required clamping forces were determined based upon the axial stress generated at maximum pressure, such that each of 8 3/8" studs required 16 ft-lbs of torque—with a safety factor of 2, the minimum torque requirement became 32 ft-lbs. This was calculated using the following torque-force equation:

$$T = \frac{F_p DK}{N}$$

where T is the torque per bolt, F_p the required preload force of the assembly, D the nominal thread diameter, K a coefficient determined by the type and state of materials used, and N the number of bolts in the assembly. For this application, K for unlubricated general steel is assumed at 0.36. In addition to clamping forces, several hardware components had to be fitted and sealed into the lid--these included the inlet and outlet ports, pressure transducer seat, viewing window seat, and hydraulic cylinder mount. As space became a premium on the lid, all parts except the transducer were custom designed.

The inlet and outlet ports were constructed of the same 6061-T6 aluminum with anodized finish, and were simply a threaded hole cut into a tapered cylinder. The ports were sealed with a bolt, torqued to hold against the maximum calculated σ_z and sealed against leaks with Barclad (Gaynor Industries, Wilmington, MA) sealing washers. Each inlet was designed with wrench flats to allow the user an effective griping method to torque the ports into the NPT-threaded mounts. National Pipe Thread (NPT) tapered threads are a standard used to effectively seal pipes without the use of O-rings and compression seals (gaskets). As NPT standard threads are torqued, they create a seal as the flanks of adjacent threads compress together (as opposed to parallel threads, which merely couple two parts). NPT threads are normally installed with thread seal tape or paste to reduce marring and galling as the threads compress. NPT threads were also used to install the high-pressure sight glass (Rayotek, HP Sight Glass 3/4") and the pressure transducer (Honeywell, FPA2000).

The hydraulic cylinder-piston assembly presented unique design challenges. Sealing was crucial, and a piston with a main piston cup seal (McMaster) and a backup O-ring (McMaster), both of Buna-N, provided the required sealing capacity (cup seal up to 3000 psi). This double layer of sealing was a key design parameter to ensure full operating pressure was realizable even under failure of one of the seals; it also allowed for convenient seal (O-ring) replacement. The cylinder and piston were machined from 17-4 PH stainless steel due to the requirement of an extremely smooth, hard surface. Additional polishing was performed on the bore to obtain a surface roughness of less than 20 μinch.

One of the major considerations given by the BPVC is the concept of "leak before burst"--simply, that the vessel will leak small amounts of fluid (reducing fluid volume and thus pressure) when stressed to failure instead of undergoing a catastrophic rupture event. In order to accommodate this standard, gasketing materials with pressure ratings equal to or less than 1000 psi (7.5 MPa) were used to a provide a passive pressure release system. These gaskets (silicone rubber, McMaster) were less than $10, so this was deemed the most cost-effective way of preventing vessel rupture. Additional system hardware safety points were installed along with the gaskets, and these are discussed in System Hardware.

System Hardware

In addition to the pressure vessel itself, all ancillary hardware--actuator mounts and operational accessories--was designed in Pro/ENGINEER Wildfire 5. Custom assemblies included the linkage hardware between the linear actuator and piston, mounting brackets for the actuator, and an attachable base for the vessel. The stepper motor, stepper drive, universal motion interface (UMI), analog to digital converter (ADC), pressure transducer and amplifier, and several power supplies were the electrical components specifically chosen to control the system.

One of the design criteria was that the system needed to be modularized; in essence, that any part of the system could be swapped for a similar component and the new whole would continue to function as required. One of the advantages of designing in modules was that many different types of linear actuator systems could drive the pressurization of the vessel, such as an MTS. While extremely precise and reliable, the cost of purchasing a material testing system is quite high. The design of the piston

linkage system, along with the geometric placement of the cylinder and piston assembly, allowed other linear actuators (stepper motor, servo) to hook up and drive the system.

This module-centric design paradigm facilitated the use of in-house available stepper motors (UltraMotion, D-B.125-HT23) which reduced startup and equipment costs. The high torque NEMA 23 motor (HT23) incorporated in this actuator had a maximum force output of 390 lbs. The vessel cylinder bore diameter, at ½", provided an additional level of safety to the system. Using the stress equation:

$$\sigma = \frac{F}{d^2 \pi / 4}$$

to calculate stress output yields a maximum stress of 2000 psi, or 13.3 MPa, which is significantly less than the burst range of the vessel. Thus, in the event of a motion control failure, the motor does not possess the necessary power to produce stress magnitudes high enough to cause rupture.

In order to mount the stepper motor, a detachable base for the vessel was constructed that allowed the attachment of a vertical support which was fitted with the motor mounting brackets. This vertical support, or spine, was designed such that it had two anchor points with the vessel, to help eliminate any rock or play in the spine and keep the piston aligned with the bore. The base was fitted with rubber spacers on the contact surfaces to increase the coefficient of friction between itself and the vessel, which allowed for the use of a long lever bar to aid in the torqueing of the lid bolts.

To incorporate pressure feedback in the system, a transducer (Honeywell, FPA2000) was installed in the lid. For the purposes of initial experiments and validation, this transducer had a pressure range of 0-200 psia (1.33 MPa absolute) and was deemed appropriate for near-future work. Another transducer (Honeywell, FPA2000) with

pressure range of 0-1500 psia (10 MPa absolute) was also purchased for higher pressure experiments. These transducers were unamplified internally, so a separate external amplifier was acquired (Honeywell, DV-10). As it was necessary to further condition and digitize the amplified signals, an inexpensive USB-mode ADC from National Instruments (NI, USB-6009) was integrated, completing the pressure feedback control system. A block diagram of the essential components is illustrated in Figure 3.3.

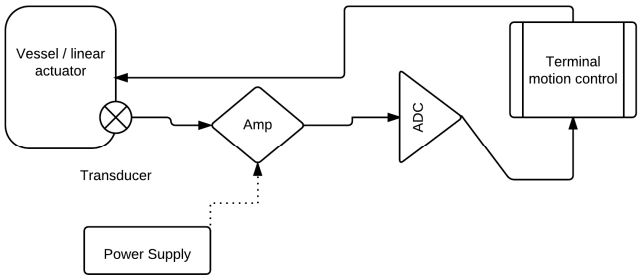

Figure 3.3: Block diagram of pressure feedback loop.

The motion control hardware was picked, as much as possible, from existing in-house units. Figure 3.4 shows a block diagram of the essential motion control system components. The UMI (National Instruments, UMI-7764) was salvaged from an existing system no longer in use and adapted to meet the requirements of the project. A custom 26-pin control cable was constructed to allow communication from the UMI to the required motor drive. The drive (Danaher, P70530) was the only purchased component

in the motion control system. It was required for its high amperage output (6.7A), necessary to enable the stepper to generate the large forces required by the project.

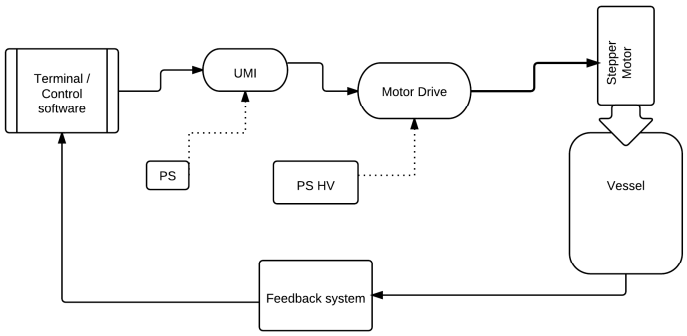

Figure 3.4: Block diagram of motion control system. PS represents power supply; UMI the universal motion interface; and PS HV a high-voltage power supply to the drive.

Operational hardware consisted of the tubing necessary for fill procedures, the waterbath used to maintain a 37° C environment within the vessel, and the various power supplies used to excite amplifiers or power components (drive and UMI). Tygon tubing was acquired in three foot sections as well as a size B hose clamp for securing a leak-proof seal around the inlet. Figure 3.5 is an image of the pressure vessel in the water bath with tubing attached. A used waterbath (Fisher, ISOTEMP110) was acquired and devoted to the purpose of keeping the testing environment at 37° C. Power supplies for

the UMI and transducer were picked from in-house units (Sensotec, 032-0070-02), while the supply for the drive was ordered from Digikey (Mean Well, LPV-100-36).

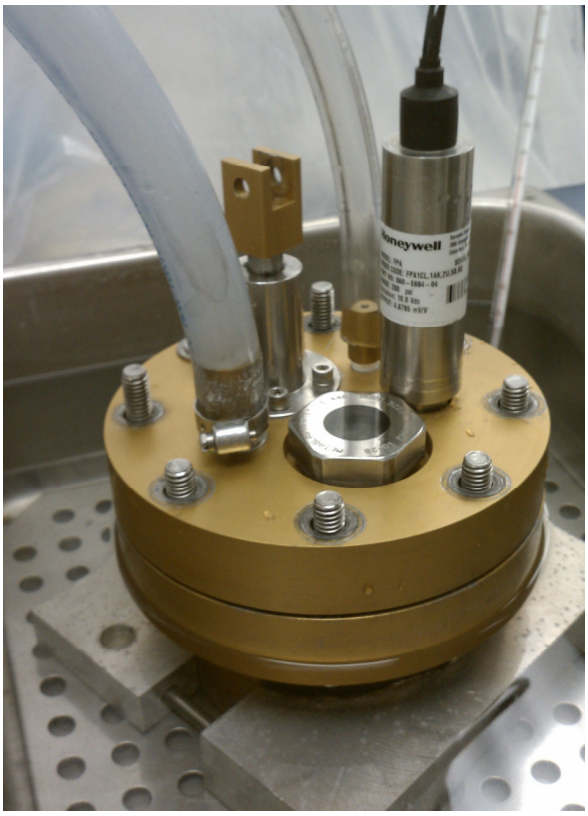

Figure 3.5: Image of ancillary hardware.

Software Control

Motion and feedback of the system was controlled with custom LabVIEW (NI, v10.0.1) code. The general coding scheme was based upon the same module-centric

paradigm as vessel and hardware construction, allowing an experienced user to replace certain code blocks with a slightly different function while not perturbing the overall control of the system. Modules were divided into sub-modules, which were further encapsulated by base virtual instruments (VIs), the functional unit of G (LabVIEW code language). Significant modules included the graphical user interface (GUI), setup procedure, motor control, runtime monitor, fault handler, and data recorder.

Software package (henceforth as MIDAS) development began, and was centrally focused, on the user interface. The creation of a simple, user-friendly, and understandable interface was paramount to the overall usability of the system. In order to reveal the most efficient interface, detailed operational steps were recorded and analyzed. Any point which did not absolutely require user intervention was automated, and those steps with required physical intervention (such as a manual jog of the motor to set limits) had extensive tool tips and dialogs; these steps were organized on the GUI in a logical top to bottom, left to right style. Options with prerequisite steps were turned off (unavailable) until the required actions had been completed. Figure 3.6 shows a flow chart of the GUI operational steps, beginning after specimen placement.

The setup (operational) module was a compilation of several sub-modules, each designed to accomplish one of the steps defined in the user interface. Referring to Figure 3.6, these steps were experimental parameter input, definition of motor runtime conditions, vessel filling, vessel priming, and waveform setup. Parameter input was simplified as much as possible; the user only had to input specimen name, any additional notes, the minimum and maximum pressures, the frequency, and the test duration. Parameters that had obvious limits or boundary conditions were coded to check for data

integrity; for example, if the minimum pressure was greater than the maximum, the user would be alerted and unable to continue until corrected.

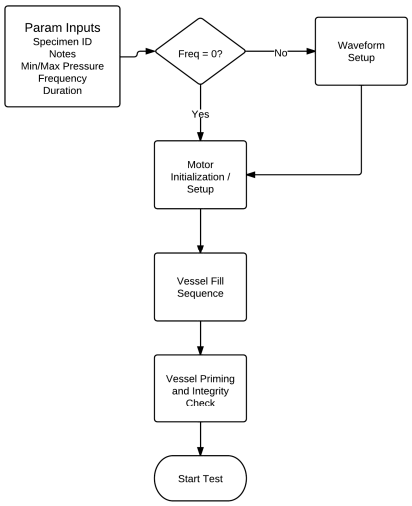

Figure 3.6: Flowchart of GUI steps. Different vertical levels indicate prerequisites, with higher steps before lower ones.

Parameter limits were also imposed, as detailed in Table 3.1. Values outside the given limits were coerced to the corresponding boundary. The subroutines in the motor runtime setup were designed to provide an extra level of protection for the components of the motion system. While technically not critical to test performance, these instruments were responsible for zeroing the motor to a reference position, set by the user, and for imposing motion limits within the motor's stroke range. These limits were customizable; for example, an experienced user could use the full two inches of stroke as boundary conditions, or if a low pressure test was run, impose a forward (compression stroke) limit

at 1 inch, effectively limiting the amount of possible compression. At the conclusion of motor setup, a prompt instructing the user how to mount the motor was displayed and execution stopped until the user confirmed mounting was complete.

Table 3.1: Parameter definitions and limits.

Parameter	**Limits**
Pressure	Min: 0.09 MPa Max: 5.0 MPa Max must be greater than min
Frequency	0-2 Hz
Duration	1-1440 min (24 hrs)
Waveform	2-4 linear components Period start pressure must equal period end pressure

The vessel fill procedure took advantage of the code reusability inherent with G; all VIs used were from the motor setup sub-module, with different user prompts. The fill sub-module guides the user in fully priming the system with pressurization fluid by filling the cylinder. The fill process is performed manually, giving the user an additional layer of control, the consequence of which was that a (recommended) buffer zone could be created between the fill level and lower (relax stroke) limit. These zones became important during the priming phase of operation setup, because they allowed the motion controllers to compensate for air pockets still existing in the system.

The priming phase consisted of cycling the vessel from maximum to minimum pressure twice. It checked system integrity by recording displacement values during each cycle, and failed if the two cycle displacements had a difference greater than 10%. If true, the user would be alerted to check all vessel hardware and search for leaks along the sealing surfaces, otherwise setup would continue to the last step of waveform generation (if appropriate). If the user inputs a target frequency greater than zero, the default waveform is triangular at the given frequency. However, the system was designed so that n-part waves could be applied, where n represents an integer indicating the number of wave constituents. Due to constraints of the motion controller (NI 7330, National Instruments), these constituents were designed as linear pieces with a target pressure (rise) and a target length (run). For initial experiments, n was set and coded for a maximum of 4 wave parts. The module was designed to allow for modification by an experienced LabVIEW user to accommodate as many subunits as desired, however.

Once the user completed waveform setup, the system waited until the START command was issued (via a virtual switch) before beginning the test. At this time, MIDAS would activate the runtime monitor, immediately followed by the motor control and data recorder modules. The runtime monitor was designed as an additional safety feature to protect the system from leaving the previously set displacement and pressure bounds, as well as a failsafe in case of sudden feedback loss. This module was the result of an iterative process that lasted several cycles, beginning with the realization that sudden ADC stalling could cause the motor controller to maximally displace the piston in an attempt to reach the preset pressure level. After several versions with a "kill" type

failsafe (ending compression but also stopping the test), a "recovery" failsafe was programmed by adding the fault handling module.

The fault module is activated only when the runtime monitor determines that a fault has occurred. Once engaged, the module forces the motor control and runtime monitor to exit and immediately halts the motor. It then issues a move command to the stepper motor back to the position it was in immediately prior to starting the test. This clears any extrema faults. While the motor movement is performed, the module directly polls the ADC device three times, with a period of 250 ms, in order to detect a stall. If the three measurements are exactly equal, this indicates a stalled ADC (even if the motor is not moving, slight noise will cause the functional ADC's readings to minutely fluctuate) and the hardware components in the feedback system are reset programmatically. This ADC check process iterates until the ADC shows dissimilar readings or three tries have been performed; in the event of unsuccessful reset, the test is suspended and the user asked to power cycle the components manually. If reset is successful, the module restarts the runtime monitor and motor control modules. It is important to note that the fault handler does not kill the data capture module, so that faults can be detected when analyzing the pressure and displacement data.

The data capture process begins immediately prior to motor control initiation, and cannot be killed except by the successful completion signal, or a system quit. Sampling is set at a fixed 15 Hz rate, which is 7.5x the maximum system frequency (2 Hz), mitigating aliasing effects in the data. An array of zeros is pre-allocated for 125% of the predicted number of samples, and is modified per data entry. Proper memory allocation practices, such as pre-allocation, were necessary due to the large amount of data captured

(108,000 64-bit integers for a two hour test). In the event the array becomes greater than 90% full (a system stall, extending testing time) the data array automatically allocates another 10% of the existing array size and appends it to the end of the current array. In addition to data capture, pressure and displacement data are sent to the GUI and displayed for the user in a scrolling chart form. On exit, the module will either save the data to a .txt file (successful completion) or dump all existing data into a .dump file (quit, failure). In the case of faults or system failure, the system automatically dumps existing data to a .fault file.

CHAPTER 4

MATERIALS AND METHODS

Figure 4.1 shows the protocols and methods in flowchart form.

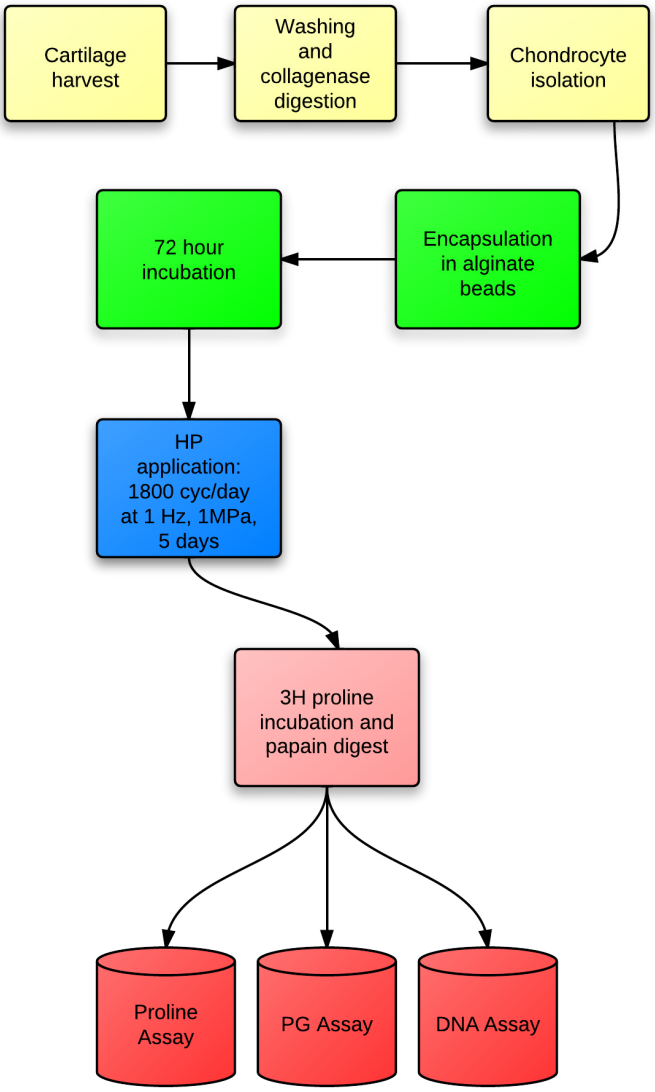

Figure 4.1: Flowchart of experimental model.

Tissue Harvest

Mature bovine knee joints were purchased from a local abattoir (Bud's Custom Meats, Riverside, IA). The knees were dissected and either shavings from the femoral condyle (lateral, medial) cut with a #22 scalpel blade (chondrocyte), or 1" x 1" x ½" explants manually sawed from the tibial plateau (CPC), were collected in a 100 ml specimen cup and washed in a solution of Hank's Balanced Salt Solution (HBSS) and Penicillin-Streptomycin-Amphotericin B at a concentration of 50 ml / 1 ml, respectively. The slices/explants were taken to a hood after collection and washed again using the same HBSS/PS+AB solution.

Chondrocyte Isolation

While the cartilage shavings were soaked for decontamination, a digestion buffer consisting of collagenase type 1 and pronase E (Sigma-Aldrich, St. Louis, MO) dissolved in culture medium (0.25 mg/ml) was pressed through a sterile filter. The culture media was Dulbecco's modified Eagle medium (DMEM) supplemented with 10% fetal bovine serum (Invitrogen, Carlsbad, CA), 100 U/ml penicillin, 100 µg/ml streptomycin, 50 µg/ml L-ascorbate, and 2.5 µg/ml Fungizone. Once filtration was complete, the buffer was placed in a large NUNC plate along with the cartilage shavings, which were further chopped into fine (1-2 mm) pieces. The cartilage was left in this solution overnight (12 ± 3 hours).

After digestion, the mixture was pipetted up and down several times to break up and homogenize the digest solution. Using a sterile 70-100 micron cell strainer, the digest was filtered into a 50 ml centrifuge tube. The filtered solution was collected and centrifuged at 3000 revolutions per minute (rpm) for five minutes. The supernatant was removed after centrifugation and the cell pellet resuspended with fresh culture medium in T-225 flasks. The total volume in each flask was 50 ml. Media was changed in the

flasks every 48 hours until cell confluency, at which point the cells were counted using hemocytometry and then passaged to new flasks.

Alginate Bead Production

Cell suspension within alginate beads essentially followed the procedure outlined by Guo[24], with alginate concentration tuned to 1.2% as performed by Kasra[34]. Alginate (Sigma Aldrich) was dissolved in phosphate buffered saline (PBS) at a concentration of 1.2% alginate (560 mg alginate in 50 ml PBS). Upon full dissolution of alginate, the mixture was sterile filtered into a 50 ml centrifuge tube.

Cell suspensions containing either chondrocytes or CPCs were spun down at 1500 rpm for five minutes and the supernatant removed. Cell pellets were resuspended in a volume of sterile 1.2% alginate solution that would yield 10 million cells / ml. The resuspension was pipetted up and down to break up the cell pellet and homogenize the solution. Using a 25 gauge needle, beads with a volume of approximately 11 µl (110k cells / bead) were dripped into a shallow culture dish containing 102 mM $CaCl_2$. The beads were left to polymerize in the solution for 5-10 minutes, after which they were washed with HBSS and transferred to culture dishes filled with culture medium.

Hydrostatic Pressurization

After a 72 hour incubation period, half of the beads were subjected to cyclic hydrostatic pressure (HP), while the second half, used as controls, remained in culture dishes and incubated absent HP. Heat-sealable polyethylene sheeting was cut into 3.5" x 7" rectangles and folded in half to create a 3.5" pouch. The pouches were washed in 70% ethanol and dried in a fume hood. Once the ethanol had evaporated, pouches were double-sealed along three sides as well as an additional diagonal corner seal. The inside

was washed once with HBSS to remove any remaining alcohol residues. Beads and a small amount of current culture media were transferred into the pouch via sterile pipette, and an additional 25 ml culture media added to the pouch. The open side of the pouch was double-sealed and corner sealed, then labeled. Each specimen's beads had a separate pouch (bag). The controls were not manipulated, as it has been shown there are no significant differences between controls placed in the vessel water bath and those remaining in culture[2]. However, several rounds of sham controls (control beads that were bagged and placed in the water bath, but not pressurized) were tested to confirm that the bagging procedure and slight temperature fluctuations in the water bath did not affect the cells.

Hydrostatic pressurization was performed using a custom designed pressure vessel and LabVIEW software. The chamber and pressurizing fluid (water) were placed in the water bath (37º C) one hour before testing in order to equilibrate them with the media in the pouches. Upon equilibrium, the pouches were placed into the chamber and sealed. Cyclic HP from 0.1-1 MPa (± 0.1 MPa) was applied as a triangle wave at a frequency of 1 Hz at 50% duty (1 Hz cycle every 2 seconds) for one hour, once per day for five days. Thus, each specimen was exposed to 1800 cycles of HP per day.

Each day after testing, specimens were removed from the pouches via sterile pipette and re-plated onto new culture dishes with fresh media. The media of controls was fully changed every day at the same time as the experimental group.

Proline Assay

The beads for proline incorporation and PG content assays were placed in fresh culture dishes containing 10 µl of tritiated proline ([H^3] proline) per 1 ml of culture

medium. After 18.5 hours, the [H^3] proline/ media solution was aspirated and the beads were washed with normal media for four hours. Following this wash, an additional 20 hour wash was performed in DMEM. Papain digestion was performed on the beads following washing in a digestion buffer of water, L-cysteine, sodium phosphate and ethylenediaminetetraacetic acid (EDTA) with 0.25 mg/ml papain (Sigma Aldrich) until the beads were fully dissolved (up to 4 hours).

The digested solution was centrifuged at 1200 rpm for 10 minutes to pellet any debris. Using a clear 24-well plate, 1ml of Optiphase Supermix (Wallac) was added to each of three wells, per specimen (triplicates). 100 µl of supernatant was added to each well from the corresponding group and mixed via pipetting. The plates were placed in the Trilux Scintillation Counter (Wallac) and Microbeta used to collect the data (counts per minute (CPM), per well).

PG Assay

The PG content assay was performed using the same supernatant as that of the proline incorporation assay. A 96 well, clear plate was used to run triplicates (three assays) of each specimen, as well as a triplicate of standards. Standards were performed with each set of PG assays. 190 µl of phosphate bovine serum albumin/EDTA (PBE) and 10 µl of supernatant were dispensed into the first row and mixed; 100 µl of this row was extracted and mixed with 100 µl PBE in the second row, and so on to form a set of 7 serial dilutions. 200 µl of Dimethylene methyl blue (DMMB) was added to each well and mixed by pipetting. Completed plates were run in a kinematic microplate reader (Molecular Devices) and optical intensity data collected via SoftMax software.

Statistical Methods

The data collected were normalized to 100k cells for equivalent comparison. This was accomplished by taking CPM or intensity data and using the following equation:

$$Q = \frac{RC_Q}{NC_R}$$

where Q is the data in normalized form, R is the data in raw form, C_Q is normalized cell count desired, N is the number of beads in the specimen, and C_R is the number of cells per bead. These data were analyzed using a one-way ANOVA (Holm-Sidak comparison method) with significance defined at $p < 0.05$.

CHAPTER 5

RESULTS

Each experimental group of chondrocytes was from a different animal (n = 5 for PG content, n = 3 for proline incorporation). Sham controls were performed on two groups of chondrocytes (n=2 for shams, see Table A1 for data). All raw data was normalized to a value representative of 100,000 cells for equal comparison purposes. Proline incorporation data is shown in Figure 5.1. The incorporation of proline in group NC1 (normal chondrocytes, group 1) had a 44% increase in the hydrostatic condition, while NC4 and NC5 showed decreases in proline incorporation (raw data can be seen in Appendix A, Table A1). There are no significant differences between any of the groups.

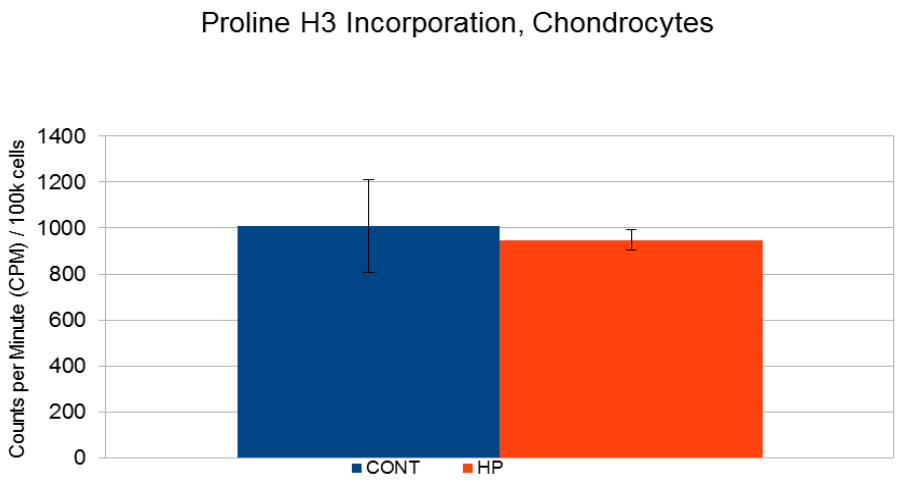

Figure 5.1: Proline incorporation of normal chondrocytes. Error bars represent the standard error of the mean.

Proteoglycan content revealed a stronger trend towards HP (HP conditions all show higher PG content), with one specimen showing an 85% increase in PG content in the hydrostatic condition; this was the same sample showing increases in proline incorporation. A second specimen showed a 61% increase in PG content. Graphical data is shown in Figure 5.2, where error bars represent the standard error of the mean. There were no significant differences between the groups.

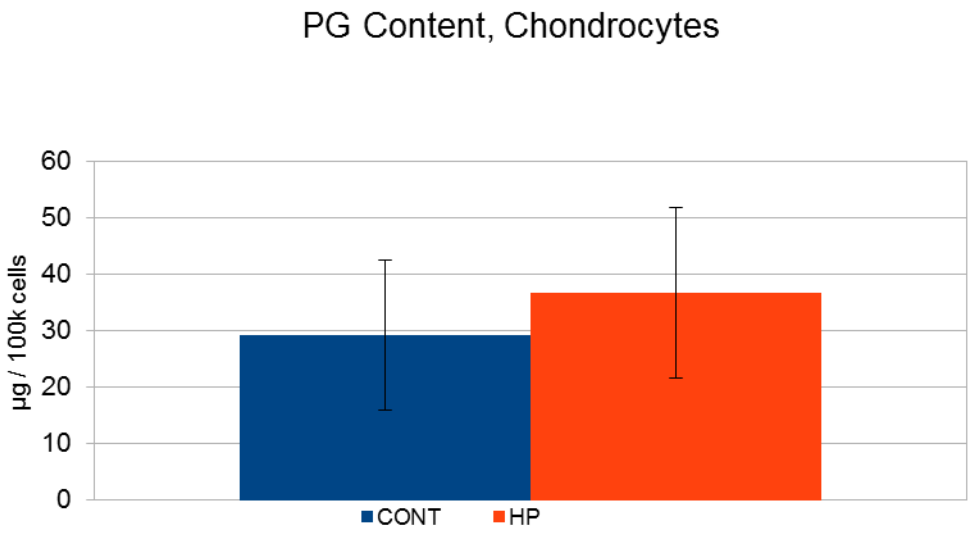

Figure 5.2: Proteoglycan content of normal chondrocytes. Control conditions (CONT), hydrostatic pressure conditions (HP). Error bars represent the standard error of the mean.

Due to large differences between the raw data sets, each specimen was further normalized to the controls to facilitate a comparison that minimized the effect of inter-

animal tissue and cell variation. Controls were set to a value of 1, and HP and sham groups scaled to a fold change value. This fold-change data is displayed in Figure 5.3. The differences between the groups are not significant.

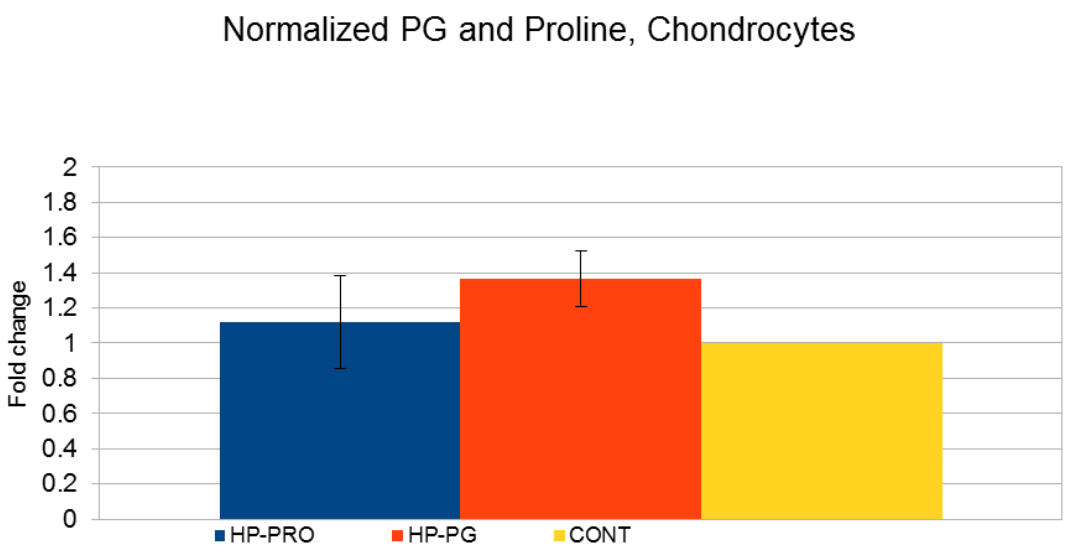

Figure 5.3: Normalized PG and proline data for normal chondrocytes. Proline and PG groups represent HP treatments, while the control (CONT) group is the baseline between the two. Error bars represent the standard error of the mean.

CHAPTER 6

DISCUSSION

The results of these preliminary experiments indicate that for the given model, there are no significant differences in the proline incorporation nor PG content between control groups that are unpressurized, and test groups which receive 1800 cycles of 1 MPa cyclic HP at 1 Hz per day. There is also no difference between sham controls and cultured controls. Thus, it appears that this loading regime/scaffold substrate combination does not cause chondrocytes to increase their matrix synthesis rate and deposition of proteins, specifically proteoglycans and collagen. There are several determining factors that are involved in the outcome of HP stimulation, and as discussed previously, any number or combination of these may significantly affect the result.

It is likely, however, that the statistical power of the experiments is merely too low to detect a significant difference. Analyzing the raw data, two of the five HP samples show a 60-85% increase in PG content, and one of five HP samples show a 44% increase in proline incorporation. This type of high sample variability is not uncommon; Meyer et al. have observed that between donors, the exact same cyclic HP treatment produced opposite results[42]. It is possible that tissues from different animals will react differently to the same stimulus, though the general trend should remain similar. Even when normalizing to each specimen's control group, the results are inconclusive. An N number of 7-10 (different animals) may provide the necessary power to resolve a difference between HP and control/sham control groups.

These experiments assume a homogeneous mixture of cells and alginate in the bead dripping phase, as well as similar-volume beads between the sample groups. While bead volumes were determined to be consistent (data not shown), and homogeneity of the alginate solution is a reasonable assumption (given proper mixing), cell numbers may change over the course of the nine day experiment. It is possible that some cells die while others escape the alginate bead; it has been shown that chondrocytes in alginate beads under cyclic HP do not change their proliferation rate[18]. However, these changes may be non-trivial; thus, beads from each group should be assayed for DNA content and the proline/PG results normalized to these findings, and not a bead volume assumption.

Assuming that these results are representative of this model, and not a statistical artifact, it may be that the alginate substrate plays a role in the non-reactivity of embedded chondrocytes. Alginate provides little in the way of cell adhesion; while this keeps chondrocytes in the ideal spherical shape, it may also lead to reduced cytoskeletal prestress and a reduced response to applied hydrostatic pressure[13], suggesting that a high HP in alginate cultures may correspond to a normal HP *in vivo*. Thus, 1 MPa of cyclic HP may simply be too small of a magnitude to show significant differences from controls. Cellular signaling also plays a role in chondrocyte mechanotransduction, and while the cell density of beads was comparable to native cartilage, a lack of cell-matrix adhesion points could lead to reduced chondrocyte communication. Elder et al. have reported similar non-reactivity when testing chondrocytes suspended in alginate beads, reporting no difference between GAG content nor proline incorporation under 5 MPa, 1 Hz HP[18]. Further, they used transmission electron microscopy (TEM) to show that

chondrocytes in alginate resided in smooth-walled pockets with little to no cell adhesion points or cell-cell contact.

The timing of the HP application may have also contributed to the lack of a difference between pressurized beads and controls. Several studies[17, 38, 47] show that a delay of 10-14 days between initial seeding and HP application result in higher PG and collagen synthesis, less HP-related cell death, and greater phenotypic stability. This amount of time was shown to allow the cells to lay down an initial matrix which may have allowed better cell attachment and a more native cell-tissue interaction, leading to a greater reaction to HP. The culture time in the current study was only 3 days, which may not have provided enough time for the cells to lay down a matrix to which they could adhere. This could have been compounded by the initial lack of attachment provided by the alginate substrate.

Future work will involve the completion of additional normal chondrocyte groups, as well as assaying the DNA content of the current set of specimens and normalizing the data accordingly. If the DNA content normalization still shows a lack of statistical power, more animals will be passed into the current experimental model, up to a maximum of ten (n=10) per group. Based upon these results, future work will either focus on optimizing the current model, or performing pilot studies on a different model (such as agarose culture and 10 day incubation). The chosen experimental model will also be used to determine the differences between the responses of chondrocytes and CPCs under hydrostatic pressure. Ultimately, the chosen model should produce cartilage constructs that have enough mechanical viability to be conditioned further via direct compression and shearing methods.

APPENDIX A

EXPERIMENTAL DATA

Table A1: Experimental data.

	Raw			**Normalized**		
Proline	Control	HP	Sham	Control	HP	Sham
NC1	627.3	905.1		1	1.443	
NC4	1095.98	900.84	1191.24	1	0.8219	1.087
NC5	1302.89	1035.44	1609.84	1	0.7947	1.2356
PG						
NC1	12.99	23.97		1	1.857	
NC2	6.65	6.58		1	0.99	
NC3	6.14	9.9		1	1.614	
NC4	48.68	57.75	42.27	1	1.186	0.868
NC5	71.81	85.44	75.04	1	1.190	1.045

Note: NC is normal chondrocyte, the numeral following indicates group number. Proline is measured in counts per minute, proteoglycan content in μg / 100k cells.

REFERENCES

1 D. D. Anderson, S. Chubinskaya, F. Guilak, J. A. Martin, T. R. Oegema, S. A. Olson, and J. A. Buckwalter, 'Post-Traumatic Osteoarthritis: Improved Understanding and Opportunities for Early Intervention', *J Orthop Res,* 29 (2011), 802-9.

2 P. Angele, J. U. Yoo, C. Smith, J. Mansour, K. J. Jepsen, M. Nerlich, and B. Johnstone, 'Cyclic Hydrostatic Pressure Enhances the Chondrogenic Phenotype of Human Mesenchymal Progenitor Cells Differentiated in Vitro', *J Orthop Res,* 21 (2003), 451-7.

3 C. W. Archer, and P. Francis-West, 'The Chondrocyte', *Int J Biochem Cell Biol,* 35 (2003), 401-4.

4 N. M. Bachrach, V. C. Mow, and F. Guilak, 'Incompressibility of the Solid Matrix of Articular Cartilage under High Hydrostatic Pressures', *J Biomech,* 31 (1998), 445-51.

5 L. Bian, D. Y. Zhai, R. L. Mauck, and J. A. Burdick, 'Coculture of Human Mesenchymal Stem Cells and Articular Chondrocytes Reduces Hypertrophy and Enhances Functional Properties of Engineered Cartilage', *Tissue Eng Part A,* 17 (2011), 1137-45.

6 K. D. Brandt, 'Response of Joint Structures to Inactivity and to Reloading after Immobilization', *Arthritis Rheum,* 49 (2003), 267-71.

7 A. N. Brown, B. S. Kim, E. Alsberg, and D. J. Mooney, 'Combining Chondrocytes and Smooth Muscle Cells to Engineer Hybrid Soft Tissue Constructs', *Tissue Eng,* 6 (2000), 297-305.

8 T. D. Brown, R. C. Johnston, C. L. Saltzman, J. L. Marsh, and J. A. Buckwalter, 'Posttraumatic Osteoarthritis: A First Estimate of Incidence, Prevalence, and Burden of Disease', *J Orthop Trauma,* 20 (2006), 739-44.

9 J. A. Buckwalter, 'Articular Cartilage Injuries', *Clin Orthop Relat Res* (2002), 21-37.

10 J. A. Buckwalter, and T. D. Brown, 'Joint Injury, Repair, and Remodeling: Roles in Post-Traumatic Osteoarthritis', *Clin Orthop Relat Res* (2004), 7-16.

11 J. A. Buckwalter, and J. A. Martin, 'Sports and Osteoarthritis', *Curr Opin Rheumatol,* 16 (2004), 634-9.

12 J. A. Buckwalter, J. A. Martin, and T. D. Brown, 'Perspectives on Chondrocyte Mechanobiology and Osteoarthritis', *Biorheology,* 43 (2006), 603-9.

13 C. S. Chen, and D. E. Ingber, 'Tensegrity and Mechanoregulation: From Skeleton to Cytoskeleton', *Osteoarthritis Cartilage,* 7 (1999), 81-94.

14 D. R. Dirschl, J. L. Marsh, J. A. Buckwalter, R. Gelberman, S. A. Olson, T. D. Brown, and A. Llinias, 'Articular Fractures', *J Am Acad Orthop Surg,* 12 (2004), 416-23.

15 G. P. Dowthwaite, J. C. Bishop, S. N. Redman, I. M. Khan, P. Rooney, D. J. Evans, L. Haughton, Z. Bayram, S. Boyer, B. Thomson, M. S. Wolfe, and C. W. Archer, 'The Surface of Articular Cartilage Contains a Progenitor Cell Population', *J Cell Sci,* 117 (2004), 889-97.

16 F. Eckstein, M. Reiser, K. H. Englmeier, and R. Putz, 'In Vivo Morphometry and Functional Analysis of Human Articular Cartilage with Quantitative Magnetic Resonance Imaging--from Image to Data, from Data to Theory', *Anat Embryol (Berl),* 203 (2001), 147-73.

17 B. D. Elder, and K. A. Athanasiou, 'Effects of Temporal Hydrostatic Pressure on Tissue-Engineered Bovine Articular Cartilage Constructs', *Tissue Eng Part A,* 15 (2009), 1151-8.

18 S. H. Elder, S. W. Sanders, W. R. McCulley, M. L. Marr, J. W. Shim, and K. A. Hasty, 'Chondrocyte Response to Cyclic Hydrostatic Pressure in Alginate Versus Pellet Culture', *J Orthop Res,* 24 (2006), 740-7.

19 S. H. Elder, J. W. Shim, A. Borazjani, H. M. Robertson, K. E. Smith, and J. N. Warnock, 'Influence of Hydrostatic and Distortional Stress on Chondroinduction', *Biorheology,* 45 (2008), 479-86.

20 I. E. Erickson, S. R. Kestle, K. H. Zellars, G. R. Dodge, J. A. Burdick, and R. L. Mauck, 'Improved Cartilage Repair Via in Vitro Pre-Maturation of Msc-Seeded Hyaluronic Acid Hydrogels', *Biomed Mater,* 7 (2012), 024110.

21 A. Fioravanti, D. Benetti, G. Coppola, and G. Collodel, 'Effect of Continuous High Hydrostatic Pressure on the Morphology and Cytoskeleton of Normal and Osteoarthritic Human Chondrocytes Cultivated in Alginate Gels', *Clin Exp Rheumatol,* 23 (2005), 847-53.

22 L. E. Freed, J. C. Marquis, R. Langer, G. Vunjak-Novakovic, and J. Emmanual, 'Composition of Cell-Polymer Cartilage Implants', *Biotechnol Bioeng,* 43 (1994), 605-14.

23 R. Gerter, J. Kruegel, and N. Miosge, 'New Insights into Cartilage Repair - the Role of Migratory Progenitor Cells in Osteoarthritis', *Matrix Biol* (2012).

24 J. F. Guo, G. W. Jourdian, and D. K. MacCallum, 'Culture and Growth Characteristics of Chondrocytes Encapsulated in Alginate Beads', *Connect Tissue Res,* 19 (1989), 277-97.

25 A. C. Hall, J. P. Urban, and K. A. Gehl, 'The Effects of Hydrostatic Pressure on Matrix Synthesis in Articular Cartilage', *J Orthop Res,* 9 (1991), 1-10.

26 U. Hansen, M. Schunke, C. Domm, N. Ioannidis, J. Hassenpflug, T. Gehrke, and B. Kurz, 'Combination of Reduced Oxygen Tension and Intermittent Hydrostatic Pressure: A Useful Tool in Articular Cartilage Tissue Engineering', *J Biomech,* 34 (2001), 941-9.

27 S. Hattori, C. Oxford, and A. H. Reddi, 'Identification of Superficial Zone Articular Chondrocyte Stem/Progenitor Cells', *Biochem Biophys Res Commun,* 358 (2007), 99-103.

28 C. A. Heath, and S. R. Magari, 'Mini-Review: Mechanical Factors Affecting Cartilage Regeneration in Vitro', *Biotechnol Bioeng,* 50 (1996), 430-7.

29 J. Heyland, K. Wiegandt, C. Goepfert, S. Nagel-Heyer, E. Ilinich, U. Schumacher, and R. Portner, 'Redifferentiation of Chondrocytes and Cartilage Formation under Intermittent Hydrostatic Pressure', *Biotechnol Lett,* 28 (2006), 1641-8.

30 J. C. Hu, and K. A. Athanasiou, 'A Self-Assembling Process in Articular Cartilage Tissue Engineering', *Tissue Eng,* 12 (2006), 969-79.

31 M. Huber, S. Trattnig, and F. Lintner, 'Anatomy, Biochemistry, and Physiology of Articular Cartilage', *Invest Radiol,* 35 (2000), 573-80.

32 S. Jia, L. Liu, W. Pan, G. Meng, C. Duan, L. Zhang, Z. Xiong, and J. Liu, 'Oriented Cartilage Extracellular Matrix-Derived Scaffold for Cartilage Tissue Engineering', *J Biosci Bioeng* (2012).

33 M. O. Jortikka, J. J. Parkkinen, R. I. Inkinen, J. Karner, H. T. Jarvelainen, L. O. Nelimarkka, M. I. Tammi, and M. J. Lammi, 'The Role of Microtubules in the Regulation of Proteoglycan Synthesis in Chondrocytes under Hydrostatic Pressure', *Arch Biochem Biophys,* 374 (2000), 172-80.

34 M. Kasra, W. D. Merryman, K. N. Loveless, V. K. Goel, J. D. Martin, and J. A. Buckwalter, 'Frequency Response of Pig Intervertebral Disc Cells Subjected to Dynamic Hydrostatic Pressure', *J Orthop Res,* 24 (2006), 1967-73.

35 I. M. Khan, R. Williams, and C. W. Archer, 'One Flew over the Progenitor's Nest: Migratory Cells Find a Home in Osteoarthritic Cartilage', *Cell Stem Cell,* 4 (2009), 282-4.

36 M. M. Knight, T. Toyoda, D. A. Lee, and D. L. Bader, 'Mechanical Compression and Hydrostatic Pressure Induce Reversible Changes in Actin Cytoskeletal Organisation in Chondrocytes in Agarose', *J Biomech,* 39 (2006), 1547-51.

37 S. Koelling, J. Kruegel, M. Irmer, J. R. Path, B. Sadowski, X. Miro, and N. Miosge, 'Migratory Chondrogenic Progenitor Cells from Repair Tissue During the Later Stages of Human Osteoarthritis', *Cell Stem Cell,* 4 (2009), 324-35.

38 T. Kunitomo, K. A. Takahashi, Y. Arai, K. Sakao, K. Honjo, M. Saito, A. Inoue, H. Tonomura, T. Morihara, O. Mazda, J. Imanishi, and T. Kubo, 'Influence of Extracellular Matrix on the Expression of Inflammatory Cytokines, Proteases, and Apoptosis-Related Genes Induced by Hydrostatic Pressure in Three-Dimensionally Cultured Chondrocytes', *J Orthop Sci,* 14 (2009), 776-83.

39 J. L. Marsh, D. P. Weigel, and D. R. Dirschl, 'Tibial Plafond Fractures. How Do These Ankles Function over Time?', *J Bone Joint Surg Am,* 85-A (2003), 287-95.

40 J. A. Martin, and J. A. Buckwalter, 'The Role of Chondrocyte Senescence in the Pathogenesis of Osteoarthritis and in Limiting Cartilage Repair', *J Bone Joint Surg Am,* 85-A Suppl 2 (2003), 106-10.

41 LLC Matweb, 'Aluminum 6061-T6; 6061-T651 ', Matweb, (2012) <http://matweb.com/search/DataSheet.aspx?MatGUID=1b8c06d0ca7c456694c7777d9e10be5b&ckck=1> [Accessed February 23 2012].

42 E. G. Meyer, C. T. Buckley, A. J. Steward, and D. J. Kelly, 'The Effect of Cyclic Hydrostatic Pressure on the Functional Development of Cartilaginous Tissues Engineered Using Bone Marrow Derived Mesenchymal Stem Cells', *J Mech Behav Biomed Mater,* 4 (2011), 1257-65.

43 K. Miyanishi, M. C. Trindade, D. P. Lindsey, G. S. Beaupre, D. R. Carter, S. B. Goodman, D. J. Schurman, and R. L. Smith, 'Dose- and Time-Dependent Effects of Cyclic Hydrostatic Pressure on Transforming Growth Factor-Beta3-Induced Chondrogenesis by Adult Human Mesenchymal Stem Cells in Vitro', *Tissue Eng,* 12 (2006), 2253-62.

44 S. Mizuno, T. Tateishi, T. Ushida, and J. Glowacki, 'Hydrostatic Fluid Pressure Enhances Matrix Synthesis and Accumulation by Bovine Chondrocytes in Three-Dimensional Culture', *J Cell Physiol,* 193 (2002), 319-27.

45 V. C. Mow, S. C. Kuei, W. M. Lai, and C. G. Armstrong, 'Biphasic Creep and Stress Relaxation of Articular Cartilage in Compression? Theory and Experiments', *J Biomech Eng,* 102 (1980), 73-84.

46 H. Muir, 'The Chondrocyte, Architect of Cartilage. Biomechanics, Structure, Function and Molecular Biology of Cartilage Matrix Macromolecules', *Bioessays,* 17 (1995), 1039-48.

47 S. Nakamura, Y. Arai, K. A. Takahashi, R. Terauchi, S. Ohashi, O. Mazda, J. Imanishi, A. Inoue, H. Tonomura, and T. Kubo, 'Hydrostatic Pressure Induces Apoptosis of Chondrocytes Cultured in Alginate Beads', *J Orthop Res,* 24 (2006), 733-9.

48 L.S. Negi, *Strength of Materials* (7 West Patel Nagar, New Delhi 110 008: Tata McGraw-Hill Publishing Company Ltd, 2008).

49 K. W. Ng, C. J. O'Conor, L. E. Kugler, J. L. Cook, G. A. Ateshian, and C. T. Hung, 'Transient Supplementation of Anabolic Growth Factors Rapidly Stimulates Matrix Synthesis in Engineered Cartilage', *Ann Biomed Eng,* 39 (2011), 2491-500.

50 K. Sauerland, R. X. Raiss, and J. Steinmeyer, 'Proteoglycan Metabolism and Viability of Articular Cartilage Explants as Modulated by the Frequency of Intermittent Loading', *Osteoarthritis Cartilage,* 11 (2003), 343-50.

51 R. M. Schulz, and A. Bader, 'Cartilage Tissue Engineering and Bioreactor Systems for the Cultivation and Stimulation of Chondrocytes', *Eur Biophys J,* 36 (2007), 539-68.

52 Dong Rim Seol, Tae-Hong Lim, James A. Martin, and University of Iowa. College of Engineering. Biomedical Engineering., 'Chondrogenic Progenitor Cell Response to Cartilage Injury and Its Application for Cartilage Repair', (Iowa City, Iowa: University of Iowa,, 2011), pp. x, 121 p.

53 J. Seror, Y. Merkher, N. Kampf, L. Collinson, A. J. Day, A. Maroudas, and J. Klein, 'Articular Cartilage Proteoglycans as Boundary Lubricants: Structure and Frictional Interaction of Surface-Attached Hyaluronan and Hyaluronan--Aggrecan Complexes', *Biomacromolecules,* 12 (2011), 3432-43.

54 M. Singh, M. Pierpoint, A. G. Mikos, and F. K. Kasper, 'Chondrogenic Differentiation of Neonatal Human Dermal Fibroblasts Encapsulated in Alginate Beads with Hydrostatic Compression under Hypoxic Conditions in the Presence of Bone Morphogenetic Protein-2', *J Biomed Mater Res A,* 98 (2011), 412-24.

55 R. L. Smith, J. Lin, M. C. Trindade, J. Shida, G. Kajiyama, T. Vu, A. R. Hoffman, M. C. van der Meulen, S. B. Goodman, D. J. Schurman, and D. R. Carter, 'Time-Dependent Effects of Intermittent Hydrostatic Pressure on Articular Chondrocyte Type Ii Collagen and Aggrecan Mrna Expression', *J Rehabil Res Dev,* 37 (2000), 153-61.

56 R. L. Smith, S. F. Rusk, B. E. Ellison, P. Wessells, K. Tsuchiya, D. R. Carter, W. E. Caler, L. J. Sandell, and D. J. Schurman, 'In Vitro Stimulation of Articular Chondrocyte Mrna and Extracellular Matrix Synthesis by Hydrostatic Pressure', *J Orthop Res,* 14 (1996), 53-60.

57 J. P. St-Pierre, L. Gan, J. Wang, R. M. Pilliar, M. D. Grynpas, and R. A. Kandel, 'The Incorporation of a Zone of Calcified Cartilage Improves the Interfacial Shear Strength between in Vitro-Formed Cartilage and the Underlying Substrate', *Acta Biomater* (2011).

58 R. A. Stockwell, 'The Cell Density of Human Articular and Costal Cartilage', *J Anat,* 101 (1967), 753-63.

59 M. Venn, and A. Maroudas, 'Chemical Composition and Swelling of Normal and Osteoarthrotic Femoral Head Cartilage. I. Chemical Composition', *Ann Rheum Dis,* 36 (1977), 121-9.

60 D. R. Wagner, D. P. Lindsey, K. W. Li, P. Tummala, S. E. Chandran, R. L. Smith, M. T. Longaker, D. R. Carter, and G. S. Beaupre, 'Hydrostatic Pressure Enhances Chondrogenic Differentiation of Human Bone Marrow Stromal Cells in Osteochondrogenic Medium', *Ann Biomed Eng,* 36 (2008), 813-20.

61 M. Wong, M. Siegrist, and K. Goodwin, 'Cyclic Tensile Strain and Cyclic Hydrostatic Pressure Differentially Regulate Expression of Hypertrophic Markers in Primary Chondrocytes', *Bone,* 33 (2003), 685-93.